Controlling the Activity of an Immobilised Molecular Catalyst by Lewis Acidity Tuning of the Support

Philip Kenyon, D. W. Justin Leung, Meng Lyu, Chunping Chen, Zoë R. Turner, Jean-Charles Buffet, Dermot O'Hare*

Chemistry Research Laboratory, Department of Chemistry, University of Oxford, 12 Mansfield Road, Oxford OX1 3TA, U.K.

ABSTRACT: The performance profile of a supported metallocene catalyst in slurry-phase ethylene polymerization can be significantly enhanced by tuning the chemical composition of the support. By employing catalyst supports derived from zinc-containing layered double hydroxides (LDHs), the slurry phase ethylene polymerization productivity of (EBI)$ZrCl_2$ (EBI = *rac*-ethylenebis(indenyl)) can be quadrupled relative to a magnesium-containing support. Productivity increases approximately linearly with zinc content of the LDH before reaching a plateau, our experiments suggest the productivity of this catalyst system is related to the overall Lewis acidity of the support surface. We have found that iron-containing LDH supports with a similar overall Lewis acidity also results in productivity enhancements, demonstrating the general nature of this phenomena.

KEYWORDS:

supported catalyst, support effect, ethylene polymerization, zirconocene, layered double hydroxide

INTRODUCTION:

Immobilization of molecular catalysts offers many possible advantages, in fine chemical

synthesis it offers the potential for recycling.[1] However, there remain several barriers to the introduction of immobilized catalysts in the fine chemicals industry, mainly associated with the increased costs of heterogenization.[2] By contrast the immobilization of homogeneous (post-)metallocene polyethylene complexes on a support is an area of great industrial importance, and therefore has been investigated thoroughly.[3-6] These supported catalysts provide an alternative to heterogeneous Ziegler-Natta and Phillips catalysts, offering access to polymers with narrower molecular weight distributions and distinct microstructures.[6] Various methods of immobilization have been reported,[4] however ion-pairing is the most common due to the predominantly cationic nature of these catalysts and the ease of immobilizing these species with the oligomeric anionic species methylaluminoxane (MAO).

A range of inorganic solids and polymeric materials have been investigated, however the most common is silica.[4, 7-9] While silica offers excellent properties in terms of size and shape control, its chemical tunability is limited.[7] Polymerization catalysis can be influenced by the concentration of surface silanols (which can be tuned *via* calcination)[10] or by functionalization of the surface with organic molecules introduced by reaction with surface silanols.[11-13] The influence of the support on the catalyst behavior, has instead been demonstrated by comparing distinct inorganic supports such as silica and alumina.[14] A systematic investigation of the influence of the support on these catalysts, therefore potentially offers an additional route to tuning the polymerisation behaviour of these catalysts.

A highly tunable class of inorganic supports are layered double hydroxides (LDH). These inorganic solids are commonly represented by the formula, $[M_{(1-x)}M'_x(OH)_2]^{a+}\,[A^{n-}_{a/n}]\cdot mH_2O$ (M and M' are most commonly divalent (e.g. Mg^{2+}) and trivalent (e.g. Al^{3+}) cations respectively, A^{n-} is an anion, and $0 < x < 1$). As such they form Brucite like layers with intercalated anions (A^{n-}) to balance the overall positive charge of the metal hydroxide sheet. LDH has previously been

used as a support for polymerization catalysts,[15-17] and can be templated onto other inorganic materials to make a range of core-shell species,[18-21] some of which have also been used as catalyst supports.[22] It has previously been shown that the choice of cations and anions have a significant influence on polymerization behaviour.

These highly tunable supports have great potential to serve as platform systems, whereby a number of different metal ions with a range of properties can be incorporated with minimal structural changes to show how physiochemical properties of the support can influence the chemistry of the immobilized catalyst. Here we demonstrate how by tuning one aspect (the nature of the divalent metal cation) the activity of an immobilized *ansa*-zirconocene complex (EBI)$ZrCl_2$ (EBI = *rac*-ethylenebis(indenyl)) can be significantly enhanced. We relate this to a fundamental property of the Lewis acidity of the support and show how the same effect can be achieved by alternatively tuning the nature of the trivalent metal cation.

RESULTS AND DISCUSSION:

Zinc and magnesium are commonly used divalent cations in LDH chemistry. To investigate what effect substituting magnesium with zinc had on catalyst activity a series of $Zn_x(Mg_{3-x})Al$-LDHs ($[(Zn_xMg_{1-x})_{0.75}Al_{0.25}(OH)_2][CO_3]_{0.125}\cdot mH_2O$) were synthesized by coprecipitation. M(II) was varied from 100 % Mg (x = 0) to 100 % Zn (x = 1), in all cases the trivalent cation (M(III)) selected was aluminum and the ratio of M(II):M(III) was fixed at 3:1. The coprecipitation pH was fixed at 10 and in all cases, the coprecipitation was carried out in the presence of Na_2CO_3 to produce carbonate containing LDHs. A comparison of the theoretical and actual values of the ratios of zinc, magnesium and aluminum for this series $Zn_x(Mg_{3-x})Al$ (where $0 \leq x \leq 3$) is given in Table 1.

The purity of the synthesized LDH can be demonstrated by the similarity of the theoretical and the actual values (Table 1), XRD patterns of the synthesized LDH (Figure 1) and from the TGA (Figure 2, for all TGA and DTGA curves see SI, Figures S3-9). The XRD patterns of all the LDHs,

show the typical Bragg reflections of an LDH ($3R_1$ polytype). No crystalline phases associated with impurities such as zinc oxide are observed, even for Zn_3Al with the additional reflections assignable to the $3R_2$ polytype.[23]

Table 1: $Zn_x(Mg_{3-x})Al$ LDHs used to investigate the influence of the divalent cation on polymerization.

Support	Theoretical Zn:Mg Ratio[a]	Experimental Zn:Mg Ratio[b]	Theoretical M(II) Zinc Content (%)[c]	Experimental M(II) Zinc Content (%)[d]	Residual Weight at 800 °C (%)[e]	Metal-metal distance *a* (Å)[f]
Mg_3Al	0:3	0:2.87	0	0	52.43	3.0576
$Zn_{0.5}Mg_{2.5}Al$	0.5:2.5	0.47:2.26	16.7	17.2	55.54	3.0632
$Zn_{0.75}Mg_{2.25}Al$	0.75:2.25	0.72:2.14	25	25.1	56.70	3.0632
$ZnMg_2Al$	1:2	0.94:1.86	33.3	33.6	57.74	3.0668
$Zn_{1.5}Mg_{1.5}Al$	1.5:1.5	1.41:1.41	50	50.0	60.62	3.0694
Zn_2MgAl	2:1	1.88:0.94	66.7	66.7	63.79	3.0736
Zn_3Al	3:0	2.87:0	100	100	67.52	3.0842

[a]Determined by ratio of metal nitrates used in coprecipitation, relative to Al. [b]Determined by ICP-MS, relative to Al. [c]Determined by ratio of metal nitrates used in coprecipitation. [d]Determined by ICP-MS. [e]Determined by TGA (30 – 800 °C, 5 $K.min^{-1}$). [f]Determined using the position of the 110 Bragg reflection in the powder XRD.

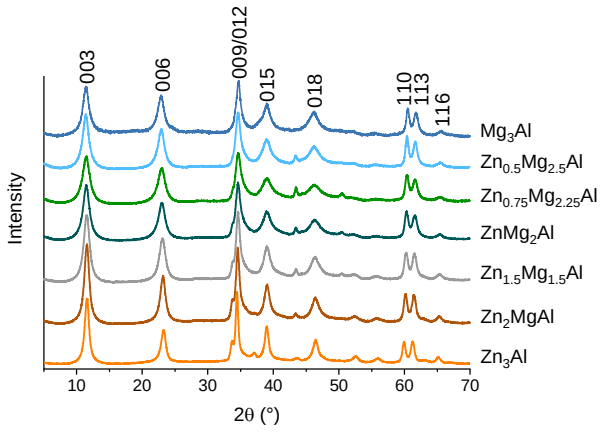

Figure 1: XRD powder patterns of $Zn_x(Mg_{3-x})Al$ LDH ($0 \leq x \leq 3$), see SI Figure S1 for *hkl* indexing of additional Bragg reflections present in Zn_3Al.

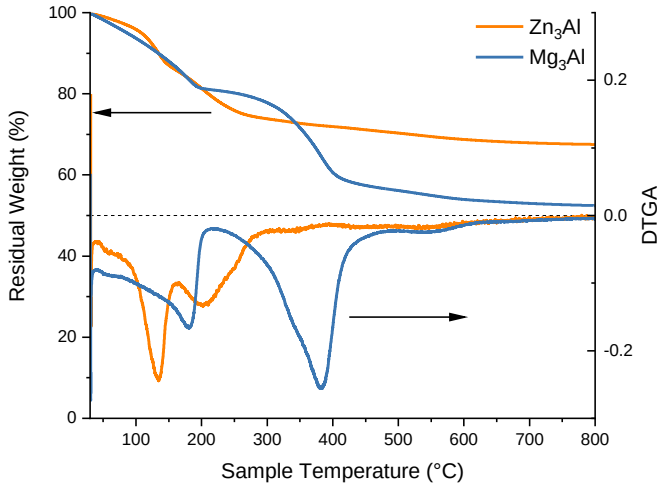

Figure 2: Selected TGA and DTGA curves for $Zn_x(Mg_{3-x})Al$ LDH (x = 0 and 3).

Using the XRD data the metal-metal distance a can be determined from the position of the 110 Bragg reflection, this shows an approximately linear trend with the met-al-metal distance increasing with the zinc content reflecting the substitution of magnesium cations with the larger zinc cation in the unit cell (see SI, Figure S2).

The TGA of Mg_3Al LDH shows a typical weight loss profile, with loss of interlayer solvents up to 200 °C, followed by the dehydroxylation of $Mg_2(OH)Al$ and Mg_3OH sites up to 400 °C.[24, 25] As previously reported, Zn_3Al LDH shows a sharp loss of interlayer solvents at lower temperatures,[26] followed by dehydroxylation at much lower temperatures,[27] as this is influenced by the nature of the metal hydroxide bond.[28] Both LDH samples show loss of mass up to 600 °C, which can be ascribed to loss of residual hydroxyl groups and carbonate anions.[25, 27] The residual weight of the LDH at 800 °C reflects the zinc content, with the magnesium being replaced by the heavier zinc ions, and the residual weight increasing approximately linearly (see SI, Figure S10).

To generate the optimum supports for metallocene immobilization, the LDHs were calcined at

400 °C for 3 hours (at a ramp rate of 10 K.min^{-1}) to generate a semi-amorphous mixed metal oxide (often referred to as a layered double oxide, LDO). LDOs still retain a low number of surface hydroxyl groups. Calcination of zinc-containing LDHs can lead to formation of small, zinc oxide crystallites at low temperature, particularly for those with high zinc content such as Zn_3Al LDH,[29] XRD of the LDO produced showed that disordered ZnO and MgO phases are produced (see SI, Figure S13). ^{27}Al-DPMAS ssNMR suggests that Al^{3+} cations are incorporated into these oxide phases as the amount of octahedral and tetrahedral aluminum changes as the zinc content of the LDO increases, with all the Al^{3+} cations being observed to be tetrahedral sites consistent with a Wurtzite (ZnO) crystal structure after calcination of Zn_3Al-LDH (see SI, Figure S14).

TGA performed under nitrogen to simulate the bulk calcination procedure (30 – 400 °C, 10 K.min^{-1} ramp rate, 3 hours at 400 °C) showed that the residual weight corresponded linearly to the zinc content (see SI, Figure S11), this suggests that for all supports, the calcination process has acted similarly with respect to dehydroxylation and loss of anions, the beginning and end points of which have been proposed to occur over a range of conditions, for example loss of CO_3^{2-} as CO_2 has been reported as beginning at temperatures ranging from below 150 to above 390 °C but is commonly assumed to be concomitant with dehydroxylation.[24, 25, 30]

The calcined support was then reacted with dried methylaluminoxane (*d*-MAO, 40 wt.%) to allow for the immobilization of a metallocene. To create the final catalyst 10 µmol of (EBI)$ZrCl_2$ was reacted with 200 mg of the *d*-MAO modified LDH support. Polymerization was carried out using 10 mg of solid catalyst (0.49 µmol Zr) with 50 mL of hexanes as diluent, 150 mg of TiBA as scavenger and 2 bar ethylene pressure. It is clear that the presence of zinc in the support has a significant impact on the productivity of the catalyst (Figure 3).

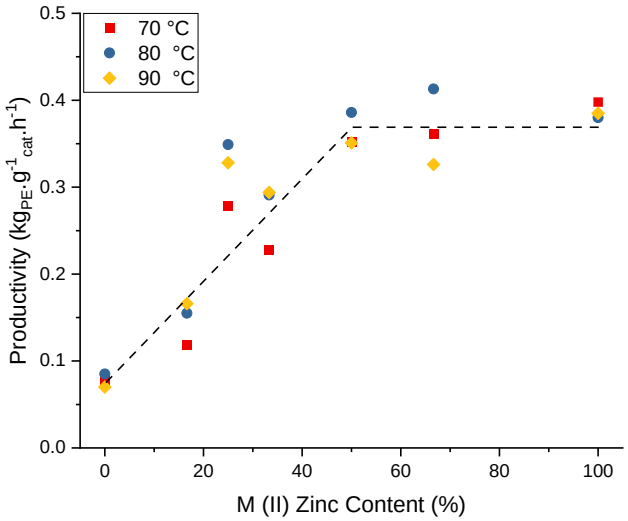

Figure 3: Productivity of catalysts using $Zn_x(Mg_{3-x})Al$ as a function of zinc content (dashed black line is a guide for the eyes).

We observe that substitution of Mg for Zn in the LDH support is associated with a large increase in catalyst productivity, the polymerization catalysts produced using Zn_3Al LDH is more than four times as active than those using Mg_3Al (0.398 vs. 0.078 $kg_{PE}.g^{-1}_{cat}.h^{-1}$ at 70 °C). For LDH supports with 0 to 50 % zinc content, productivity increases almost linearly with zinc content with 25 % zinc content being a slight exception. By contrast there is almost no change in productivity for catalysts using LDHs with between 50 to 100 % zinc content.

It is important to note that for all the supports the polymer produced is broadly comparable, having a melting point consistent with high-density polyethylene and GPC showing minimal change in molecular weight on going from Mg_3Al to Zn_3Al LDH (Figure 4).

In order to investigate the origins of this very dramatic change in productivity the physicochemical nature of the surface of the supports was investigated. The N_2 Brunauer-Emmett-Teller (BET) surface area of the LDOs was determined and it showed that there was an almost linear decrease in surface area with zinc content that cannot be accounted for just with the increased mass of zinc (see SI, Figure S18). This decrease in surface area with zinc content is likely due to the increasing instability of dehydrated zinc LDH,[26] which leads to the

collapse of the layered structures prior to dehydroxylation (at temperatures as low as 150 °C) resulting in significant loss of surface area.

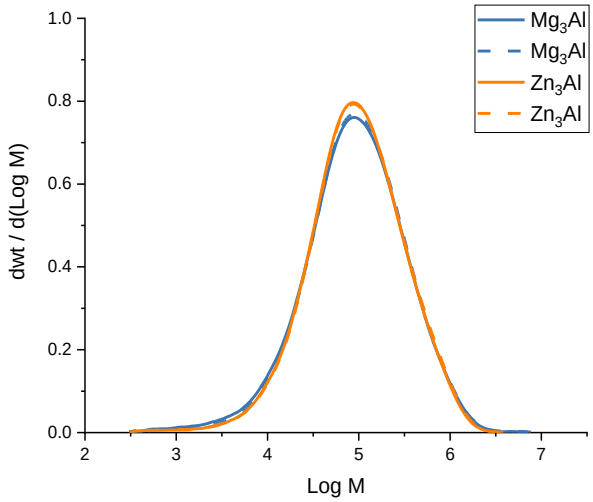

Figure 4: Molecular weight distribution of polyethylene produced using catalysts with Mg_3Al LDH and Zn_3Al LDH as supports at 70 °C as determined by GPC. Measured in duplicate, dashed line is second measurement.

The one exception to this trend is for the support based on 25 % zinc content LDH, where the surface area of the LDO is significantly higher than would be expected. This exception can be explained by a change in morphology of this support with the initial LDH being formed from smaller crystallites due to being unable to incorporate more zinc atoms into the unit cell. Evidence for this can be seen in the powder XRD patterns, the change in *a,* which is almost linear with zinc content shows no change on increasing from 16.7 to 25 %, the nature of the crystallite domains can also be studied by use of Scherrer equation (see SI, Table S1 for details). Crucially, these smaller crystallites consist of the fewest layers and so less surface area is lost when the layered structure collapses at low temperatures.

As the introduction of the more electronegative Zn^{2+} cations has led to an increase in activity the acid-base properties of the LDOs was also investigated. This was carried out using Temperature Programmed Desorption (TPD), the binding of ammonia to in-situ calcined

supports (under N_2, 30-400 °C, 10 K.min^{-1} ramp rate, 3 hours at 400 °C) was studied. Previous studies suggest ammonia is adsorbed onto LDO surfaces by two classes of interactions (see Figure 5).[31]

Prior FT-IR studies suggest that sites that bind ammonia purely through a hydrogen bond (Type A) are only stable below 200 °C, while sites which incorporate both a hydrogen bond and a dative interaction (Type B) persist at higher temperature even under vacuum.[31] These features are distinct in the TPD curve of Mg_3Al LDO (see Figure 5). For the zinc containing samples, the TPD curves obtained were deconvoluted into two broad features, and based on the ratio of these features the total number of sites were split into "Type A" and "Type B" sites (for further information on deconvolution see the SI). This was then combined with the surface area measurements to determine the concentration of each type of site per unit surface area (see Figure 6).

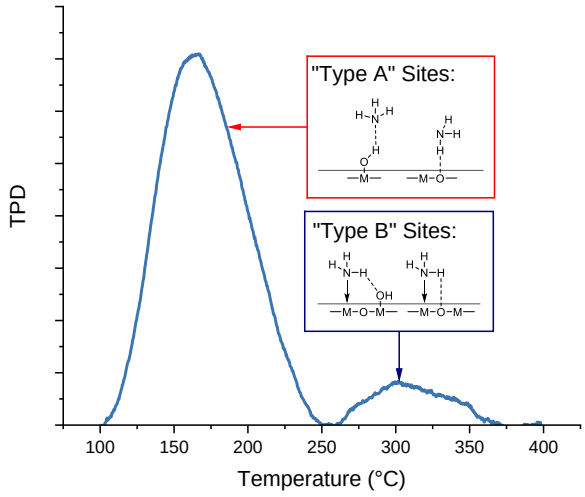

Figure 5: TPD curve of ammonia on Mg_3Al LDO, which shows the two distinct classes of interaction present between ammonia and the surface ("Type A" and "Type B").

The overall amount of ammonia that can interact with the LDO increases significantly per unit surface area for zinc containing LDOs. The additional ammonia is bound by a "medium strength" acidic site, which is typical for LDO doped with transition metals.[32] Studies on the

influence of solvent on the acidity and basicity of LDO, suggest that sites of this strength are Lewis acidic and are capable of binding solvents such as ethanol and acetone.[33] Typically for Mg_3Al LDO, Lewis acidic sites are based at Al^{3+} cations, but other divalent cations (Ni^{2+}) have been shown to provide an LDO with some Lewis acidic character.[31] The concentration of "Type B" sites which feature a Lewis acidic interaction between ammonia and the metal oxide surface increases linearly up to approximately 50 % zinc content, before remaining relatively constant (Figure 6). This corresponds qualitatively to the trend observed with catalyst productivity, and a plot of acidic site concentration against productivity at 90 °C shows a surprisingly good fit (R^2 = 0.98, see SI, Figure S23), although the higher activity of the support based on a 25 % zinc content LDH must be excluded, due to the higher surface area of this sample and the subsequent overall higher number of Lewis acidic sites (see SI, Figures S18 and S22).

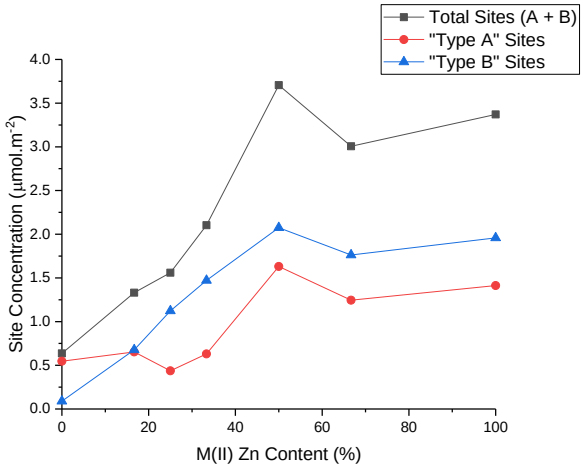

Figure 6: Change in number of sites as determined by TPD with zinc content and the number of acidic and basic sites obtained by deconvolution of TPD curves.

As activity increases we observed minimal influence on the nature of the polyethylene produced, it is likely that the number of active sites involved in polymerization at any given time is increasing. This could be due to a change in ionization efficiency or, more likely, due to

197 a change in the nature of the ion pair formed, lowering barriers to insertion. For metallocene
198 mediated polymerization the number of concurrent active sites are typically low (<30 % of
199 zirconium centers)[34] and can be influenced by the activator.[35] Previous studies suggest
200 that the presence of more Lewis acidic species in a support changes how methylaluminoxane
201 (MAO) and aluminum alkyls graft to a protic surface.[36] Studies on MAO in solution have
202 shown that exchange[37] or removal of aluminum alkyls[38] and the presence of donors can
203 change the nature of the activating site of MAO.[39]. We presume that the change in surface
204 properties leads to changes in the MAO structure which in turn leads to an enhanced activity
205 by increasing the number of catalytic centers.[40] Further study of the precise structural
206 changes is hindered by the complex nature of MAO, which is further modified in
207 composition[41] and structure[42] by drying and then how it interacts with non-periodic
208 supports.
209 We have investigated if the overall acid-base balance of the support is in fact a unifying
210 phenomenon that directly influences the performance of MAO/metallocene supported
211 catalysts. The acid-base properties of the LDO was varied by substitution of the Al^{3+} with Fe^{3+} in
212 the LDH structure, after calcination of Mg_3Fe LDH the resultant LDO showed an increased
213 concentration of Lewis acidic “Type B” sites. Polymerization catalysts based on this support
214 showed an enhanced activity (0.262 $kg_{PE}.g^{-1}_{cat}.h^{-1}$ at 70 °C) for ethylene polymerization (Figure
215 7) without changing polymer properties as determined by GPC (Figure 8).

216 These results show that these dramatic increases in productivity can be achieved by varying
217 either the M^{2+} or M^{3+} metal sites in the parent LDH. This is despite the much lower number of
218 M^{3+} sites present in an LDH and the fact that upon calcination, M^{3+} cations migrate out of the
219 initial layered structure meaning that the number and concentrations of M^{3+} and M^{2+} cations in
220 an LDO are quite distinct and not easily compared. [24]

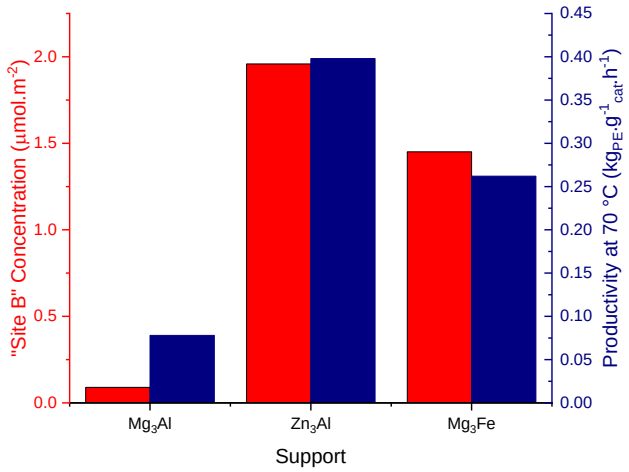

221

222 Figure 7: Ethylene polymerization productivity (70 °C), for catalysts based on various calcined

223 LDH supports and the concentration of Lewis acidic “Type B” sites.

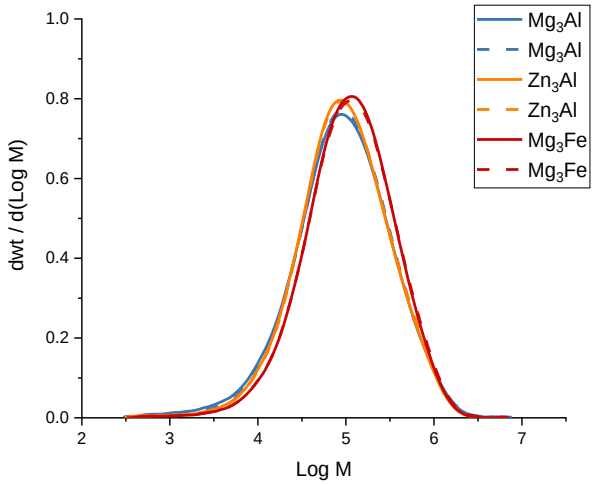

224

225 Figure 8: Molecular weight distribution of polyethylene produced using catalysts based on

226 various LDH supports at 70 °C as determined by GPC. Measured in duplicate, dashed line is

227 second measurement.

228 In summary we have shown the potential of mixed metal oxides (LDOs), derived from LDHs as

229 highly tunable inorganic supports for immobilized molecular catalysts. We demonstrate that

230 the nature of the active species in [(EBI)$ZrCl_2$]based ethylene polymerization catalysis can be

231 positively influenced by controlling the underlying acidity-basicity of the support. We are able

232 to achieve fourfold higher polymer productivity without altering the nature of the

polyethylene produced by simply altering the composition of the support.

This work should facililate a deeper understanding of how the chemical properties of supports used in industry (such as silica) could be tuned to increase their Lewis acidity and enhance the catalytic behavior of immobilized molecular catalysts.

EXPERIMENTAL:

All air-sensitive chemistry was carried out under an inert atmosphere using Schlenk line or glove-box techniques. Toluene and n-hexanes were collected from an MBraun SPS, degassed on a Schlenk line and stored over a potassium mirror for at least 12 hours before use. *d*-MAO used was dried Axion CA1330 provided by Chemtura, dried on a Schlenk line and then stored in a glove-box before use. (EBI)$ZrCl_2$ (STREM Chemicals) and TiBA (Aldrich) were stored in a glovebox prior to use. $Al(NO_3)_3{\cdot}9H_2O$ (99.999 % trace metals), $Mg(NO_3)_2{\cdot}6H_2O$ (99.999 % trace metals) and $Zn(NO_3)_2{\cdot}6H_2O$ (99.999 % trace metals), NaOH (>98 %, pellets), ethanol (>99.8 %) and pentanes (>99 %) were purchased from Aldrich and used as received.

Synthesis of $Zn_x(Mg_{3-x})Al$ LDH:

25 mmol $Al(NO_3)_3{\cdot}9H_2O$ and the appropriate amounts of $Mg(NO_3)_2{\cdot}6H_2O$ and $Zn(NO_3)_2{\cdot}6H_2O$ (75 mmol in total) were dissolved in 100 mL deionised water. This was then added at 100 $mL.h^{-1}$ to a sodium carbonate solution (12.5 mmol in 100 mL deionised water), throughout the addition the pH was monitored and the solution was maintained at pH 10 using 5 M NaOH. After the addition was complete the white suspension was stirred overnight (18 hours). The white solid was then filtered off and washed with deionised water until the filtrate was neutral. The white solid was then washed with 1 litre of ethanol, before resuspending the solid in 600 mL ethanol and stirring for four hours. The white solid was then collected by filtration, washed with 400 mL ethanol and dried overnight in a vacuum oven (<30 mBar, R.T.).

Vacuum Calcination of $Zn_x(Mg_{3-x})Al$ LDH:

500 mg of $Zn_x(Mg_{3-x})Al$ LDH was placed in a ceramic crucible, which was then placed in a quartz

tube. This tube was placed in a tube furnace, connected to a schlenk line and evacuated. Once a suitably low vacuum was reached (< 2 x10^{-1} mBar) the sample was heated to 400 °C at a heating rate of 10 K.min^{-1}, once the furnace reached 400 °C this temperature was maintained for 3 hours. The tube was under dynamic vacuum throughout the calcination and after calcination the tube was sealed and brought into a glovebox where the calcined supports [$Zn_x(Mg_{3-x})Al$ (400 °C, 3 h, 10 K.min^{-1})] were stored.

Synthesis of Catalyst Support [$Zn_x(Mg_{3-x})Al$ (400 °C, 3 h, 10 K.min^{-1})/40 wt.% *d*-MAO]:

250 mg of calcined support $Zn_x(Mg_{3-x})Al$ (400 °C, 3 h, 10 K.min^{-1}) and 100 mg *d*-MAO were weighed out and mixed as solids. Toluene (50 mL) was then added and the sample was heated to 80 °C. To ensure an even distribution of *d*-MAO on the support the suspension was swirled continuously for 15 minutes and then swirled every 5 minutes for 105 minutes. After 2 hours, the suspension was allowed to cool and the toluene was filtered off. The wet solid was dried under vacuum and the catalyst support [$Zn_x(Mg_{3-x})Al$ (400 °C, 3 h, 10 K.min^{-1})/40 wt.% *d*-MAO] stored in a glovebox.

Synthesis of Catalyst [$Zn_x(Mg_{3-x})Al$ (400 °C, 3 h, 10 K.min^{-1})/40 wt.% *d*-MAO/(EBI)$ZrCl_2$]:

200 mg of catalyst support [$Zn_x(Mg_{3-x})Al$ (400 °C, 3 h, 10 K.min^{-1})/40 wt.% *d*-MAO] and 4.2 mg (EBI)$ZrCl_2$ (10 µmol Zr, approx. 100:1 $Al_{[MAO]}$:Zr) were weighed out and mixed as solids. Toluene (15 mL) was then added and the sample heated to 60 °C. To ensure an even distribution of (EBI)$ZrCl_2$ on the catalyst support, the suspension was swirled as toluene was added and swirled continuously for 15 minutes and then swirled every 5 minutes for 45 minutes. After 1 hour, the suspension was allowed to cool and the toluene was decanted. The wet solid was dried under vacuum and the catalyst [$Zn_x(Mg_{3-x})Al$ (400 °C, 3 h, 10 K.min^{-1})/40 wt.% *d*-MAO/(EBI)$ZrCl_2$] stored in a glovebox.

Material Characterisation:

Powder X-ray diffraction (PXRD) analysis was carried out using a PANAnalytical X'Pert Pro

Diffractometer in scanning mode using Cu Kα radiation (α1= 1.540598 Å, α2 = 1.544426 Å) in reflection mode at 40 kV and 40 mA. The samples were packed on stainless steel holders which can result in peaks at 43.36, 44.29, and 50.51° but which did not interfere with the analysis. Signals between 2θ = 2 - 70° were recorded with step size 0.0167°. LDO samples were packed in the glovebox and were run immediately after bringing out the glovebox, no evidence of reconstruction was observed.

Thermogravimetric analyses (TGA) were performed under a nitrogen atmosphere using a Perkin Elmer TGA 8000. The weight change was recorded from 30 – 800 °C (5 $K.min^{-1}$). For calcination under nitrogen, the weight change was recorded from 30 – 400 °C (10 $K.min^{-1}$) and over the 3 hour hold period.

Elemental analysis by ICP-MS was carried out by Dr. Alaa Abdul-Sada at the University of Sussex. Analyses were conducted on 20-30 mg samples digested in conc. nitric acid and diluted. Each solution was analysed three times.

Solid state NMR were run on a Bruker Avance III HD solid state NMR equipped with a 9.4 T magnet, LDO samples were packed in the glovebox to prevent reconstruction to LDH.

Brunauer-Emmett-Teller (BET) method analysis was carried out using a Micromeritics 3Flex. LDO samples were weighed out in the glovebox and a check-seal fitted to prevent reconstruction. The N2 adsorption and desorption of samples were taken at -196 °C.

Prior to measurements with TPD, the LDH was calcined in-situ (to prevent reconstruction) under He. An amount of LDH was used so that after calcination there was >100 mg of LDO, based on the residual weight after calcination under N_2 at 400 °C as determined by TGA. TPD traces were recorded on a Micrometrics AutoChem II 2920 Chemisorption Analyser equipped with a thermal conductivity detector (TCD). The sample (>100 mg) was loaded in a quartz U-tube and purged with He (50 $cm^3.min^{-1}$) at room temperature for 10 minutes. This flow of helium was maintained while the temperature was raised to 400 °C using a ramp rate of 10

K.min^{-1} and held at this temperature for 3 hours, before cooling to 100 °C (10 K.min^{-1}). 10 % NH_3 in He gas (50 cm^3.min^1) was then flowed over the sample for 1 hour. Physically adsorbed NH_3 was then removed by flowing helium (50 cm^3.min^{-1}) over the sample for 1 hour. For the desorption step the sample was heated to 400 °C at a rate of 1 K.min^{-1} under a helium flow (50 cm^3.min^{-1}) with a sampling rate of 1 measurement per second.

Polymerisation Procedure:

Polymerisations were run in duplicate, if results were not consistent (defined here as within 10 % of the mean) a third polymerisation was carried out and the average value reported is that of the two consistent runs. If the third polymerisation was consistent with both original runs, or if after three runs no consistent results were obtained the average value reported is that of all three runs. In a glovebox, approx. 150 mg of TiBA was dissolved in 10 mL n-hexanes and added to a 150 mL ampoule and 10 mg of catalyst was then added. A further 40 mL of n-hexanes was then added, and the ampoule sealed and brought out of the glovebox. The ampoule was cycled on to a Schlenk line, heated to the desired temperature using an oil bath and stirred using a magnetic stirrer bar at 1000 rpm. The ampoule was carefully evacuated, and then pressurised to 2 Bar with ethylene. Polymerisation was carried out for 30 minutes, after which the ampoule was vented carefully, and the polymer isolated by filtration and washed with pentanes (50 mL) before air drying.

Polymer Characterisation:

HT-GPC were carried out by AS-Norner, each sample was run in duplicate on a high temperature gel permeation chromatograph with a IR5 infrared detector (GPC-IR5) Samples were dissolved in trichlorobenzene (TCB) with 300 ppm of 3,5-di-*tert*-butyl-4-hydroxytoluene (BHT) at 160 °C for 90 minutes and filtered with a 10 µm filter. Samples were run using TCB (300 ppm BHT) at a flow rate of 0.5 mL.min^{-1} as a mobile phase with 1 mg/mL BHT added as a flow rate marker. The GPC column and detector were set at 145 and 160 °C respectively.

Differential scanning calorimetry was carried out on a Perkin Elmer 4000 DSC, calibrated using indium at a scan rate of 20 K.min^{-1}. Samples were heated to 180 °C at 20 K.min^{-1} to remove thermal history held at 180 °C for a minute before cooling to 30 °C (20 K.min^{-1}), after holding for a minute the sample was again heated to 180 °C (20 K.min^{-1}) to record the melting point.

ACKNOWLEDGEMENTS:

Funding by SCG Chemicals Co., Ltd., Thailand is gratefully acknowledged. Dr. Alaa Abdul-Sada (University of Sussx) is thanked for running ICP-MS. Dr. Nicholas H. Rees (University of Oxford) is thanked for running solid state NMR. Dr Dana-Georgiana Crivoi (University of Oxford) is thanked for providing a sample of Mg_3Fe-LDH. Ms. Liv Thobru and Ms. Sara Herum (AS Norner) are thanked for GPC measurements.

REFERENCES:

[1] D.J. Cole-Hamilton, Homogeneous catalysis--new approaches to catalyst separation, recovery, and recycling, Science, 299 (2003) 1702-1706.

[2] S. Hübner, J.G. de Vries, V. Farina, Why Does Industry Not Use Immobilized Transition Metal Complexes as Catalysts?, Advanced Synthesis & Catalysis, 358 (2016) 3-25.

[3] G.G. Hlatky, Heterogeneous single-site catalysts for olefin polymerization, Chemical Reviews, 100 (2000) 1347-1376.

[4] J.R. Severn, J.C. Chadwick, R. Duchateau, N. Friederichs, "Bound but not gagged"--immobilizing single-site alpha-olefin polymerization catalysts, Chemical Reviews, 105 (2005) 4073-4147.

[5] M.C. Baier, M.A. Zuideveld, S. Mecking, Post-metallocenes in the industrial production of polyolefins, Angewandte Chemie, 53 (2014) 9722-9744.

[6] D.W. Sauter, M. Taoufik, C. Boisson, Polyolefins, a Success Story, Polymers, 9 (2017) 185-198.

[7] J.R. Severn, Methylaluminoxane (MAO), Silica and a Complex: The "Holy Trinity" of Supported Single-site Catalysts, in: J.R. Severn;, J.C. Chadwick (Eds.) Tailor-Made Polymers Via Immobilization of Alpha-Olefin Polymerization Catalysts, Wiley-VCH, 2008, pp. 95-138.

[8] M.E.Z. Velthoen, A. Munoz-Murillo, A. Bouhmadi, M. Cecius, S. Diefenbach, B.M. Weckhuysen, The Multifaceted Role of Methylaluminoxane in Metallocene-Based Olefin Polymerization Catalysis, Macromolecules, 51 (2018) 343-355.

[9] M.E.Z. Velthoen, J.M. Boereboom, R.E. Bulo, B.M. Weckhuysen, Insights into the activation of silica-supported metallocene olefin polymerization catalysts by methylaluminoxane, Catalysis Today, 334 (2019) 223-230.

[10] M.A. Bashir, T. Vancompernolle, R.M. Gauvin, L. Delevoye, N. Merle, V. Monteil, M. Taoufik, T.F.L. McKenna, C. Boisson, Silica/MAO/(*n*-BuCp)$_2$ZrCl$_2$ catalyst: effect of support dehydroxylation temperature on the grafting of MAO and ethylene polymerization, Catalysis Science & Technology, 6 (2016) 2962-2974.

[11] J.S. Lee, Y.S. Ko, Control of the molecular structure of ethylene-1-hexene copolymer by surface functionalization of SBA-15 with different compositions of amine groups, Journal of Molecular Catalysis A: Chemical, 386 (2014) 120-125.

[12] E.G. Barrera, F.C. Stedile, R. Brambilla, J.H.Z. dos Santos, Broadening molecular weight polyethylene distribution by tailoring the silica surface environment on supported metallocenes, Applied Surface Science, 393 (2017) 357-363.

[13] E.G. Barrera, J.H.Z. dos Santos, Designing polyethylene characteristics by modification of the support for FI catalyst, Molecular Catalysis., 434 (2017) 1-6.

[14] R. Van Grieken, A. Carrero, I. Suarez, B. Paredes, Ethylene polymerization over supported MAO/(nBuCp)2ZrCl2 catalysts: Influence of support properties, European Polymer Journal, 43 (2007) 1267-1277.

[15] F.A. He, L.M. Zhang, Organo-modified ZnAl layered double hydroxide as new catalyst support for the ethylene polymerization, J Colloid Interface Sci, 315 (2007) 439-444.

[16] J.-C. Buffet, Z.R. Turner, R.T. Cooper, D. O'Hare, Ethylene polymerisation using solid catalysts based on layered double hydroxides, Polymer Chemistry, 6 (2015) 2493-2503.

[17] J.-C. Buffet, N. Wanna, T.A.Q. Arnold, E.K. Gibson, P.P. Wells, Q. Wang, J. Tantirungrotechai, D. O'Hare, Highly Tunable Catalyst Supports for Single-Site Ethylene Polymerization, Chemistry of Materials, 27 (2015) 1495-1501.

[18] C. Chen, R. Felton, J.-C. Buffet, D. O'Hare, Core-shell SiO2@LDHs with tuneable size, composition and morphology, Chemical Communications, 51 (2015) 3462-3465.

[19] C. Chen, C.F.H. Byles, J.-C. Buffet, N.H. Rees, Y. Wu, D. O'Hare, Core-shell zeolite@aqueous miscible organic-layered double hydroxides, Chemical Science, 7 (2016) 1457-1461.

[20] W.L.J. Kwok, D.G. Crivoi, C. Chen, J.-C. Buffet, D. O'Hare, Silica@layered double hydroxide core-shell hybrid materials, Dalton transactions, 47 (2017) 143-149.

[21] M. Lyu, C.P. Chen, J.-C. Buffet, D. O'Hare, A facile synthesis of layered double hydroxide based core@shell hybrid materials, New J Chem, 44 (2020) 10095-10101.

[22] J.-C. Buffet, C.F. Byles, R. Felton, C. Chen, D. O'Hare, Metallocene supported core@LDH catalysts for slurry phase ethylene polymerisation, Chemical Communications, 52 (2016) 4076-4079.

[23] D.G. Evans, R.C.T. Slade, Structural Aspects of Layered Double Hydroxides, in: X. Duan, D.G. Evans (Eds.) Layered Double Hydroxides, Springer, Berlin, Heidelberg, 2005, pp. 1-87.

403 [24] M. Bellotto, B. Rebours, O. Clause, J. Lynch, D. Bazin, E. Elkaïm, Hydrotalcite
404 Decomposition Mechanism: A Clue to the Structure and Reactivity of Spinel-like Mixed Oxides,
405 The Journal of Physical Chemistry, 100 (1996) 8535-8542.
406 [25] W. Yang, Y. Kim, P.K.T. Liu, M. Sahimi, T.T. Tsotsis, A study by in situ techniques of the
407 thermal evolution of the structure of a Mg–Al–CO3 layered double hydroxide, Chemical
408 Engineering Science, 57 (2002) 2945-2953.
409 [26] G.M. Lombardo, G.C. Pappalardo, F. Costantino, U. Costantino, M. Sisani, Thermal Effects
410 on Mixed Metal (Zn/Al) Layered Double Hydroxides: Direct Modeling of the X-Ray Powder
411 Diffraction Line Shape Through Molecular Dynamics Simulations, Chemistry of Materials, 20
412 (2008) 5585-5592.
413 [27] T. Montanari, M. Sisani, M. Nocchetti, R. Vivani, M.C.H. Delgado, G. Ramis, G. Busca, U.
414 Costantino, Zinc–aluminum hydrotalcites as precursors of basic catalysts: Preparation,
415 characterization and study of the activation of methanol, Catalysis Today, 152 (2010) 104-109.
416 [28] G. Yu, Y. Zhou, R. Yang, M. Wang, L. Shen, Y. Li, N. Xue, X. Guo, W. Ding, L. Peng,
417 Dehydration and Dehydroxylation of Layered Double Hydroxides: New Insights from Solid-
418 State NMR and FT-IR Studies of Deuterated Samples, The Journal of Physical Chemistry C, 119
419 (2015) 12325-12334.
420 [29] X. Zhao, F. Zhang, S. Xu, D.G. Evans, X. Duan, From Layered Double Hydroxides to ZnO-
421 based Mixed Metal Oxides by Thermal Decomposition: Transformation Mechanism and UV-
422 Blocking Properties of the Product, Chemistry of Materials, 22 (2010) 3933-3942.
423 [30] M.J. Hudson, S. Carlino, D.C. Apperley, Thermal conversion of a layered (Mg/Al) double
424 hydroxide to the oxide, Journal of Materials Chemistry, 5 (1995) 323-329.
425 [31] F. Prinetto, G. Ghiotti, R. Durand, D. Tichit, Investigation of Acid−Base Properties of
426 Catalysts Obtained from Layered Double Hydroxides, The Journal of Physical Chemistry B, 104
427 (2000) 11117-11126.

[32] O.D. Pavel, D. Tichit, I.-C. Marcu, Acido-basic and catalytic properties of transition-metal containing Mg–Al hydrotalcites and their corresponding mixed oxides, Appl. Clay. Sci, 61 (2012) 52-58.

[33] D.W.J. Leung, C. Chen, J.C. Buffet, D. O'Hare, Correlations of acidity-basicity of solvent treated layered double hydroxides/oxides and their CO2 capture performance, Dalton transactions, 49 (2020) 9306-9311.

[34] M. Bochmann, The Chemistry of Catalyst Activation: The Case of Group 4 Polymerization Catalysts, Organometallics, 29 (2010) 4711-4740.

[35] F. Ghiotto, C. Pateraki, J.R. Severn, N. Friederichs, M. Bochmann, Rapid evaluation of catalysts and MAO activators by kinetics: what controls polymer molecular weight and activity in metallocene/MAO catalysts?, Dalton Trans, 42 (2013) 9040-9048.

[36] H.M. Moura, N.L. Gibbons, S.A. Miller, H.O. Pastore, 2D-aluminum-modified solids as simultaneous support and cocatalyst for in situ polymerizations of olefins, Journal of Catalysis, 362 (2018) 129-145.

[37] H.S. Zijlstra, A. Joshi, M. Linnolahti, S. Collins, J.S. McIndoe, Modifying methylalumoxane via alkyl exchange, Dalton transactions, 47 (2018) 17291-17298.

[38] F. Zaccaria, C. Zuccaccia, R. Cipullo, P.H.M. Budzelaar, A. Macchioni, V. Busico, C. Ehm, On the Nature of the Lewis Acidic Sites in “TMA-Free” Phenol-Modified Methylaluminoxane, European Journal of Inorganic Chemistry, 2020 (2020) 1088-1095.

[39] F. Zaccaria, P.H.M. Budzelaar, R. Cipullo, C. Zuccaccia, A. Macchioni, V. Busico, C. Ehm, Reactivity Trends of Lewis Acidic Sites in Methylaluminoxane and Some of Its Modifications, Inorganic Chemistry, 59 (2020) 5751-5759.

[40] N. Tymińska, E. Zurek, DFT-D Investigation of Active and Dormant Methylaluminoxane (MAO) Species Grafted onto a Magnesium Dichloride Cluster: A Model Study of Supported MAO, ACS Catalysis, 5 (2015) 6989-6998.

[41] J.-N. Pédeutour, K. Radhakrishnan, H. Cramail, A. Deffieux, Use of “TMA-depleted” MAO for the activation of zirconocenes in olefin polymerization, Journal of Molecular Catalysis A: Chemical, 185 (2002) 119-125.

[42] L. Rocchigiani, V. Busico, A. Pastore, A. Macchioni, Probing the interactions between all components of the catalytic pool for homogeneous olefin polymerisation by diffusion NMR spectroscopy, Dalton transactions, 42 (2013) 9104-9111.